# Geomatic methods applied to the study of the fronts of Johnsons and Hurd Glaciers (Livingston Island, Antarctica) from 1957 to 2013.

Ricardo Rodríguez[1], Julián Aguirre[2], Andrés Díez[2], Marina Álvarez[3], Pedro Rodríguez[4].

(1) Departamento de Señales, Sistemas y Radiocomunicaciones. ETSI de Telecomunicación. Universidad Politécnica de Madrid.
(2) Departamento de Ingeniería Topográfica y Cartografía. ETSI en Topografía, Geodesia y Cartografía. Universidad Politécnica de Madrid.
(3) Departamento de Lenguajes y Sistemas Informáticos e Ingeniería de Software. ETS de Ingenieros Informáticos. Universidad Politécnica de Madrid.
(4) Departamento de Matemática Aplicada. ETSI de Telecomunicación. Universidad de Málaga.

## Abstract

The surveying of glacier fronts combines different geomatics measurement techniques. Aerial photographs and satellite images can be used for determinate the glacier terminus line. If the glacier front is easily accessible, the classic survey using total station or theodolite, GNSS (Global Navigation Satellite System) techniques, laser-scanner or close range photogrammetry are possible. When the accessibility to glaciers is not easy, close range photogrammetry proves to be useful, cheap and fast. In this paper, a methodology that combines photogrammetric methods and other techniques for the snout of the Johnsons Glacier (inaccessible) is studied. The images obtained from the front in 2013, come from a non-metric digital camera; its georeferencing to a global coordinate system is performed by measuring points GNSS support in accessible areas of the glacier front side and applying methods of direct intersection in inaccessible points of the front, taking measurements with theodolite. The result of observations obtained with different geomatics measurement techniques, were applied to study the temporal evolution (1957-2014) of the position of the Johnsons glacier front and the position of the Argentina, Las Palmas and Sally Rocks lobes (Hurd glacier).

**Link to the data repository:** http://doi.pangaea.de/10.1594/PANGAEA.845379

## Study area and previous works

Hurd Glacier and Johnsons Glacier are located in the Hurd peninsula (Navarro et al., 2011) in the southwest of Livingston Island. Livingston Island is an Antarctic island in the South Shetland Islands, Western Antarctica lying between Greenwich Island and Snow Islands. Johnsons Glacier shows the terminus of a typical tidewater glacier, calving small icebergs into Johnsons Dock, while Hurd Glacier lobes (Argentina, Las Palmas and Sally Rocks) are land-terminating glaciers (Figure 1). Johnsons Glacier snout is continuously changing with an estimation of 50 meters per year of glacier movement near terminus area (Rodríguez, 2014). Ice velocity near terminus areas of Hurd Glacier is around 5 meters per year (Molina *et al.*, 2007).

The previous work carried with data collection fronts under study are summarized as follows:

- DOCU 1: Flight made by the British Antarctic Survey (BAS) in December 1957. A total of 5 frames (X26FID0052130, X26FID0052131, X26FID0052132, X26FID0052160 and X26FID0052161) are selected to study all of the glacier fronts.
- DOCU 2: Flight made by the United Kindom Hydrographic Office (UKHO) in January 1990. A total of 3 frames (0097, 0098 and 0099) are selected for the study of the entire glacier fronts.
- DOCU 3: Photogrammetric survey (metric camera) from the top of the glacier front Johnsons in 1999 by the University of Barcelona (Palà et al., 1999).

- DOCU 4: Satellite photograph obtained by the Quickbird system in January 2010 for the Hurd Peninsula.
- DOCU 5: Satellite photograph obtained by the Quickbird system in February 2007 for the Hurd Peninsula.
- DOCU 6: Inventory of data (2000-2012) by the Group of Numerical Simulation in Science and Engineering of the Polytechnic University of Madrid (GSNCI). These observations are made with GNSS techniques and theodolite and exclude the position of the glacier front Johnsons.
- DOCU 7: Photogrammetric survey (non-metric camera) of the front wall of Johnsons Glacier conducted in February 2013.


*Figure 1. Situation of the Johnsons and Hurd glaciers, location of the major landforms and situation of the Spanish Antarctic Base Juan Carlos I. Base map scale 1: 25000 Geographic Service of the Army in 1991.*

**The Photogrammetry**

Photogrammetry has been defined by the American Society for Photogrammetry and Remote Sensing as the art, science, and technology of obtaining reliable information about physical objects and the environment through processes of recording, measuring, and interpreting photographic images and patterns of recorded radiant electromagnetic energy and other phenomena. The photographs are most often aerial (taken from an airborne vehicle), but terrestrial photos (taken from earth-based cameras) and satellite imagery are also used. Photogrammetry lets obtain three-dimensional information from pictures using stereoscopic vision provided by two different points of view (Wolf, 1983).

The fundamental principle used by photogrammetry is triangulation. By taking photographs from at least two different locations, so-called "lines of sight" can be developed from each camera to points on the object. These lines of sight (sometimes called rays owing to their optical nature) are mathematically intersected to produce the 3-dimensional coordinates of the points of interest. Triangulation is also the principle used by theodolites for coordinate measurement. Resection is the procedure used to determine the final position and aiming (called the orientation) of the camera when a picture is taken. Typically all the points that are seen and known in XYZ in the image are used to determine this orientation. For a strong resection, you should have at least more than ten well-distributed points in each photograph. If your measurement does not have this many points, or they are not well distributed, it is recommendable to add points (Kraus, 1993).

If the XYZ coordinates of the points on the object are known, we can compute the camera's orientation. It is important to realize that both the position and aiming direction of the camera are needed. It is not sufficient to know only the camera's position since the camera could be located in the same place but be aimed in any direction. Consequently, we must know the camera's position which is defined by three coordinates, and where it is aimed which is defined by three angles. Thus, although three values are needed to define a target point (three coordinates for its position), we need six values to define a picture (three coordinates for position, and three angles for the aiming direction). It is typical of photographs from amateur cameras that the theoretical central projection is significantly deformed by lens and film distortion. These influences can be taken into account in a bundle block adjustment by introducing correction polynomials in the observation equations, whose coefficients are determined in the adjustment. Such and adjustment is called a bundle block adjustment with additional parameters or with self-calibration (Kraus, 2007). The distortion varies with the distance of each point to the center of the optical axis. The most commonly used approach is to decompose to correct distortion in their radial components and tangential (Brown, 1971). In practice, the radial distortion $\Delta r$ is much larger than the tangential distortion so that only the first, which is expressed by the equation [1] for a point coordinate image (x, y) is ignored.

$$\begin{aligned} \Delta r &= k_1 r^3 + k_2 r^5 + k_3 r^7 \\ r &= \sqrt{(x - x_0)^2 + (y - y_0)^2}, \end{aligned} \qquad [1]$$

where $k_i$ are the coefficients of radial distortion $(x_0, y_0)$ are the coordinates of PPS in the image plane and $\Delta r$ is the radial distortion to the point considered.

Once calculated systematic errors and how to correct them and to obtain three-dimensional information from two-dimensional featuring photography, photogrammetry part of the solution that provides stereoscopic vision, in which one stage photographically recorded from two different view with a common coating, three-dimensionally can be played directly through spatial intersection producing each pairing of homologous rays appearing in both images. The procedure would be the following (Figure 2):

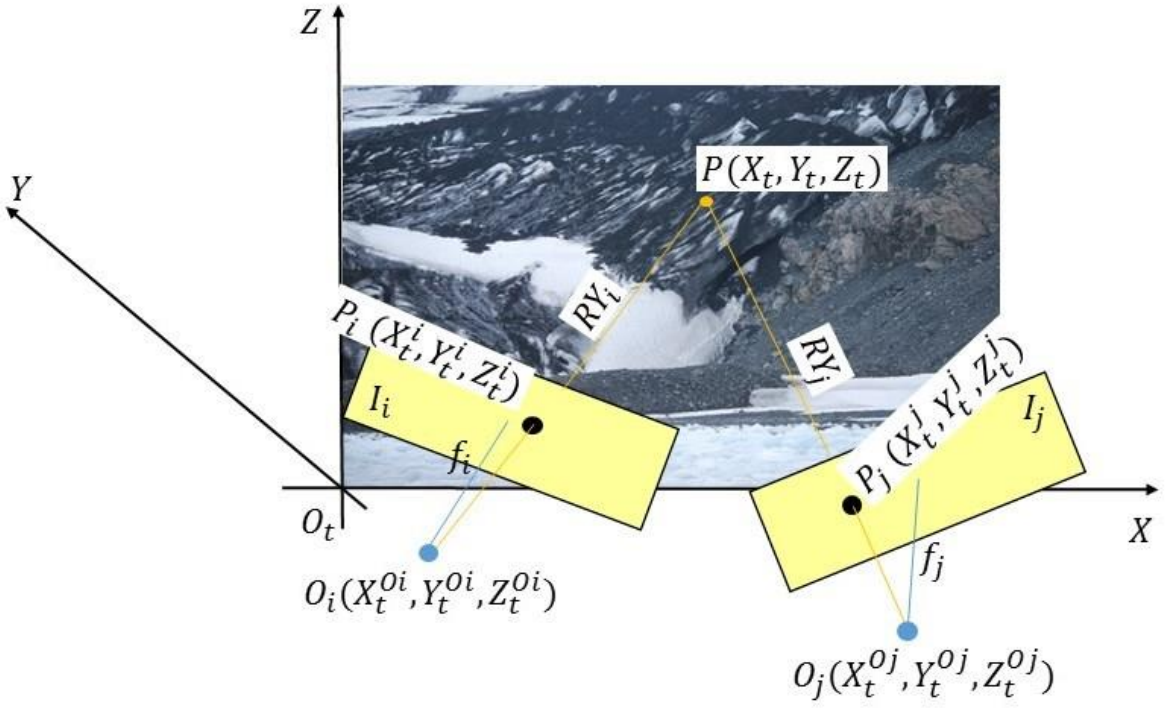


*Figure 2. Representation of point P in each of the photographs. Thus, one can calculate the unknown point coordinates in a reference system from flat photographs taken from two different points of view.*

- A terrestrial reference system $R_t$ with $O_t$ center, which is the surface you want to measure and containing the point $P$ with coordinates $(X_t, Y_t, Z_t)$ in this reference system is fixed.
- Two photographs are made from different viewpoints in this surface from $O_i\left(X_t^{O_i}, Y_t^{O_i}, Z_t^{O_i}\right)$ and from $O_j\left(X_t^{O_j}, Y_t^{O_j}, Z_t^{O_j}\right)$ (referred to $R_t$ coordinate reference system).
- Point P is represented in each of the photographs for their projections $P_i\,(X_t^i, Y_t^i, Z_t^i)$ and $P_j\,(X_t^j, Y_t^j, Z_t^j)$ (referred to $R_t$ coordinate reference system).

All this can be expressed by the so-called collinearity conditions (Kraus, 2000) which states that the center of projection, an image point and corresponding on the ground, are in the same line. The equations determining the point $P$ (whose coordinates are intended to determine), the point $P_i$ and the center of projection $O_i$ are in the same line. In like manner, the point $P$, the point $P_j$ and the center of projection $O_j$ are collinear. From the above it follows that the points $P$, $P_i$, $P_j$, $O_i$ y $O_j$ are all in the same plane, allowing us to calculate the coordinates of any point $P$ in the reference system $O_tXYZ$, by applying transformations spatial similarity (Kraus, 2007).

**Photogrammetry with non-metric camera**

To take measurements from Johnsons Glacier (February 2013), a non-metric DSLR (Digital Single-Lens Reflex) camera was used (Nikon D60). This is a typical digital camera (10 MP), not much expensive, and without excessive loss of accuracy. Obviously, its implementation requires a photogrammetric calibration, which allow to know with sufficient accuracy the internal geometry of the camera (internal orientation). Using equation [1], $k_i$ coefficients and calibrated focal length must be calculated during the calibration process.

a) Photogrammetric support

The work took place in February 2013, with fewer clouds and high visibility in the area (more than 500 m). Several control points were established making a network with permanent bases near Johnsons Glacier (see Figure 3, B1000, B2000 and B3000). In this case, these bases were measured using GNSS techniques ($\sigma_{xy} = 0{,}005\ m; \sigma_z = 0{,}008\ m$). In this case, we used Trimble 5700 GPS.

In addition, six control points were measured by the same technique at the end of the glacier, near lateral moraines (points P100, P200, P300, P400, P500 and P600 in Figure 3, $\sigma_{xy} = 0{,}011\ m; \sigma_z = 0{,}015\ m$). These points are materialized on the ground with red flags over snow. These "red points" are very easy to locate in photographs.

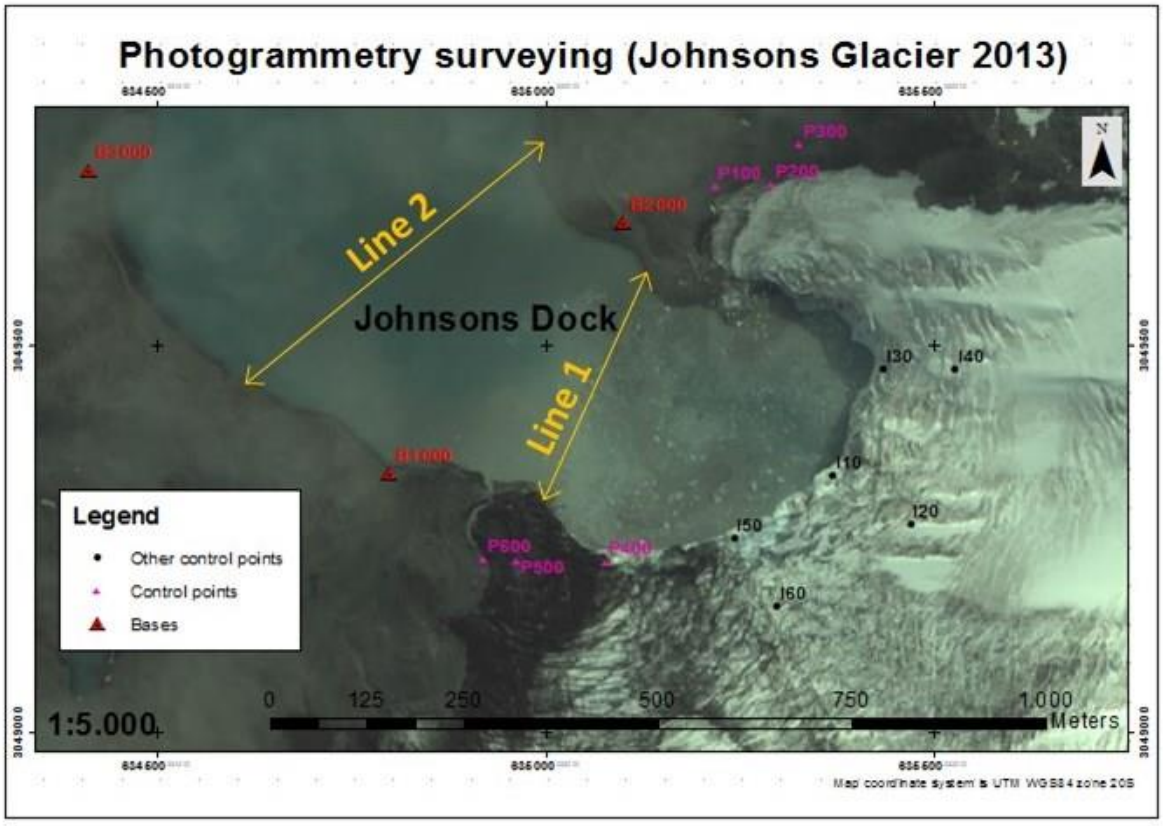


*Figure 3. Map of the B1000, B2000, B3000 bases, P100, P200, P300, P400, P500, P600 control points and I10, I20, I30, I40, I50, I60 points. In big red triangles, bases measured using GNSS techniques where theodolite was placed, in magenta triangles control points measured using GNSS techniques and finally black points (other control points) measured using direct intersection method. Line 1 and line 2 represent the track for zodiac from where the pictures were taken.*

Finally using a Wild Heerbrugg T1 theodolite, control points I10, I20, I30, I40, I50, I60 (inaccessible points) were measured. We placed theodolite above B1000, B2000 and B3000 to observe the rest of the bases, I10, I20, I30, I40, I50 and I60 to calculate control point coordinates ($\sigma_{xy} = 0{,}17\ m; \sigma_z = 0{,}30\ m$), using direct intersection method by resection from the three bases, allowing to have some redundancy in the observations (Domínguez, 1993). Previous to measures some pictures from the front of the glacier were taken to select optimal position for control points. These points had to be visible from bases (B1000, B2000 and B3000). T1 theodolite does not allow the measurement of distances, so only angle measurements were taken.

b) Shooting

As already mentioned, the camera used is a DSLR camera (Nikon D60 with lens 55-200mm AF-S DX 10 MP). The only possibility of taking pictures (normal photogrammetry) perpendicular to the front of the glacier (Figure 3) is to use a zodiac (line 1 and line 2 in Figure 3) and taking images from it. Two parallel glacier front passes took place; the first at a distance of approximately 400 m (line 1), with a focal length of 95 mm and focus to infinity. The second took place at a distance of 700 m from the glacier front with the same focal length and focus to infinity. The overlap was upper than 95%, in addition to have good quality.

To grow the number of control points over the glacier, we took more pictures from a place near P500. These photographs were taken with a focal length of 130 mm and focus to infinity. In this case we mounted the camera on a tripod and we placed in the ground to take pictures using convergent photogrammetry. Then we obtained coordinates for more control points (about 20 new points). It was also observed that in these photographs appeared stakes (EJ06, EJ36 and EJ37) identified points on the glacier (measured with GNSS techniques) (Navarro *et al.* 2013).

c) Calibration

Calibration is the first phase taking place in the office, before or after making the photographic field, but respecting the same parameters. We chose for previous calibration measures a building named "Mirador", located on the street Princesa de Eboli in Madrid, which was ideal configuration for this project (Figure 4). This building also has a large open space at the front, allowing a distance similar that used in photographic shots from the Johnsons Glacier (400 meters); this distance also makes it easy to measure the corners of the windows that will be needed in the calibration grid, using a total station. For forming the corners of the reticle windows situated in a lower horizontal line, an upper horizontal line, two central horizontal lines and three vertical lines leaving a dot pattern, as can be observed in Figure 4, were chosen. We had not access to the building plans, so we decided to use this configuration to make calibration.

We chose to determine the coordinates using angular measurements because the total station did not allow to measure distances exceeding 100 m. We applied the methodology of direct intersection (Dominguez, 1993) to determinate the coordinates of all points. Observations were made from two stations simultaneously, providing one of arbitrary local coordinates for the other station coordinates and all grid points. The coordinates of the second station were obtained with an error of 12 mm. In this process we used "Leica Geoffice" software to obtain all grid points with a mean square error of 53 mm, eliminating the points whose residues exceeded this magnitude.

We calibrated the camera for three focal lengths (85, 95 and 130 mm). We used the coordinates to obtain $k_i$ coefficients, position for PPS and finally calibrated focal length using a hundred of points (see equation [1] and Table 1).

c) Preparing images

One of the problems of work in extreme environments is that they do not allow the repetition of field observations, so a lot of errors are detected in office. It is very important to take as much information as possible during observations (of course a big number of pictures). That is why the first thing to realize is a selection of the necessary photographic peer models with an overlap of 80%.

A particular operation in the process of this project has been to correct distortion of all photographs using internal orientation parameters and generating a new set of corrected images of distortion (see Figure 5a and Figure 5b), so that may be brought into any photogrammetric program without matter what type of distortion model used.

*Figure 4. View of the facade of the building Mirador used for the calibration of non-metric camera used in photographic shots of Johnsons glacier front. Yellow, the measured points by using a total station.*

| Focal mm | Points | $x_0$ | $y_0$ | $k_1$ | $k_2$ | $k_3$ | $\sigma$ | $\sigma_{max}$ |
|---|---|---|---|---|---|---|---|---|
| 85,23 | 102 | 1975 px | 608 px | 1.25213889313851E-08 | -4.53330480188616E-15 | 4.48262617928856E-22 | 1 px | 15 px |
| 94,28 | 102 | 2043 px | 602 px | 1.18819659796645E-08 | -4.07129365804265E-15 | 3.78566248003642E-22 | 1 px | 13 px |
| 131,50 | 102 | 2017 px | 544 px | 1.20656410994392E-08 | -4.04403355146344E-15 | 3.68227991661486E-22 | 2 px | 20 px |

*Table 1. Coefficients of radial distortion and position for PPS. Two last columns show the mean square error for radial distortion and maximum error for radial distortion respectively. We considered 102 points for the polynomial adjustment. The first column shows the value for calibrated focal length (mm).*

d) Calculation of ground coordinates

With these photographs as a starting point (pictures free of radial distortion), collinearity conditions were applied, using the known support points obtained in the process of photogrammetric ground coordinates to obtain the parameters of different transformations (Helmert 3D transformations) which can obtain the ground coordinates of any point of the photographs. At the end, we obtained a total of 10 pictures to make 9 models ($\sigma_{xy} = 0{,}70\ m; \sigma_z = 0{,}55\ m$). Notice that in this case altimetry error is less than planimetry error because XZ plane is parallel to the front of the glacier (Figure 2) so that the maximum error corresponds to planimetry.

Once all parameters are calculated from different transformations, photographs are introduced together with these parameters in an own software that allows the photogrammetric restitution, without artificial stereoscopic vision (see Figure 6) using semi-automatic correlation (Luhmann *et al.*, 2006).

*Figure 5a. Original image obtained with no metric camera.*

*Figure 5b. The rectified image after applying the distortion function. It can be seen in the lower left corner of the image, an area affected by the radial distortion.*

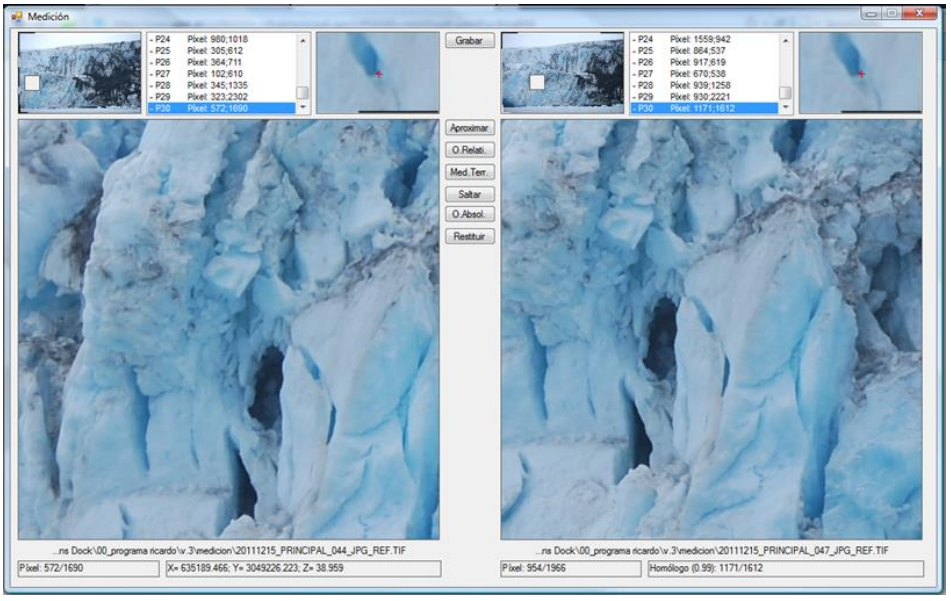


*Figure 6. Main screen of the software developed for photogrammetric restitution. This software does not require artificial stereoscopic vision and for the restitution by locating points in both images. Clicking on an item in the frame on the left, locate the point in the right using automatic correlation. This software has been developed by these authors.*

The Johnsons Glacier front has two main lines for restitution. The top one of the front and the bottom line (intersection with the sea that is defined as snout). This glacier has large amount of crevasses (Figure 7b) so it is easy to use automatic correlation. With a total of 180000 points returned by automatic correlation, orthophoto is shown in Figure 7b and restitution with principal lines of crevasses is shown in Figure 7a.

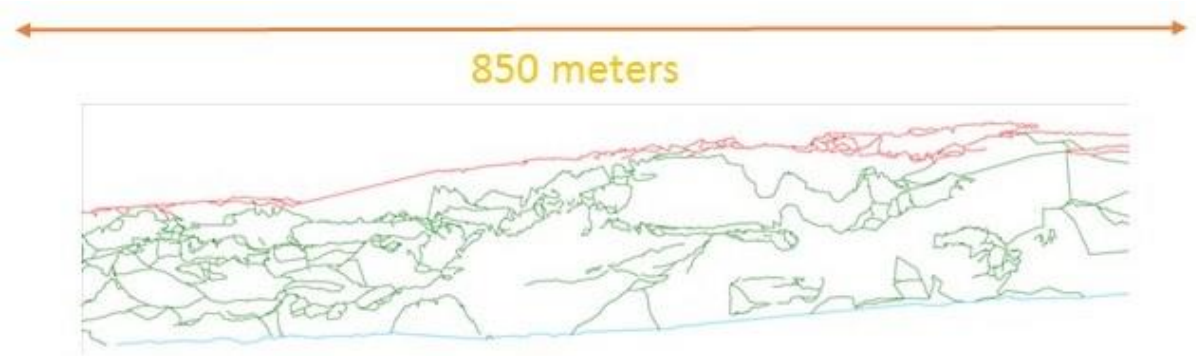


*Figure 7a. Up and red, superior front line (Johnsons Glacier) obtained by photogrammetric restitution. Down and blue, the bottom line (intersection with the sea).*

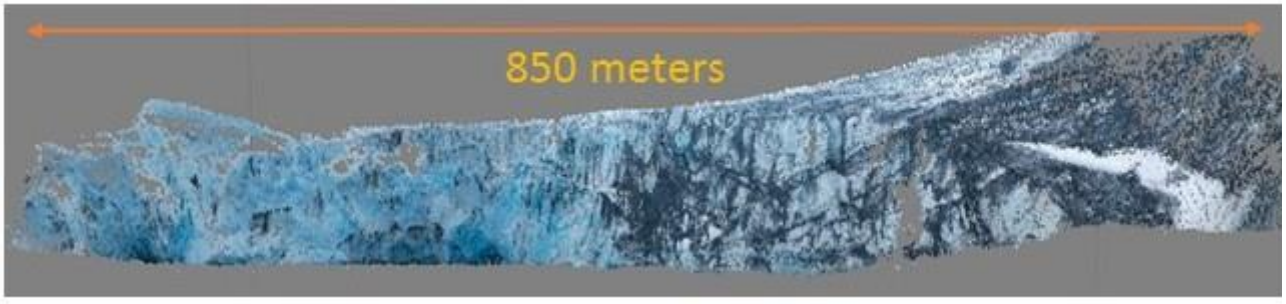


*Figure 7b. Orthophoto for Johnsons Glacier front. This point cloud has 180000 point obtained by automatic correlation.*

**Compiling data**

As seen above, the data obtained using photogrammetry from the Johnsons Glacier front, combined with data obtained using other methodologies (both the same compared to others) is use to study the temporal evolution of different fronts glaciers.

The first data are from December 26, 1957 (DOCU 1) and come from a photogrammetric flight performed metric camera to a flight altitude of 13,500 feet, with a metric camera IX Eagle Mk I and a nominal focal of 153.19 mm, which once restored using the Digi3D software, allows to obtain the position of the different glacier fronts, including the Johnsons Glacier (see Table 2). Some previous work (Molina *et al.*, 2007) use these same photographs for 3D restitution but in this study, we use only the pictures to get planimetry al level sea so that the accuracy is better. Using the certificate of calibration for IX Eagle Mk I the authors have rectified photos and then, they have georeferenced photograms X26FID0052160 and X26FID0052131 using ARCGIS with an 8 parameters transformation. In fact this flight started at the end of 1956 but it was not completed (Rodríguez, 2014).

In January 1990 (DOCU 2) turned to make another photogrammetric flight, also with metric camera. In this case, using a helicopter based on the ship HMS Endurance, to a flight altitude of 10,000 feet, with a metric camera RMK A 15/23 and a nominal focal length of 153 mm. Once restored it using the same Digi3D software, the position of the different glacier fronts is obtained, including the Jonhsons Glacier (see Table 3).

The photogrammetric survey of Johnsons Glacier front made in 1999 (DOCU 3) with metric camera from the University of Barcelona, is not considered since it corresponds to the upper front line and not to its intersection with the sea that is the line of interest (in this paper we have considered this line as the terminus line of the Johnsons Glacier).

In January 2010 a full image was captured by the Quickbird image system (DOCU 4) that covers the entire work area. It is a raster file format GEOTIFF UTM 20S on the ellipsoid WGS84. Its original name is 10JAN29132854-P2AS-052832138010_01_P001.TIF and was obtained from http://www.euspaceimaging.com with reference ID "101001000B044C00". It is a black and white image with 16-bit digital values, but actually quantization levels are reduced to 11 bits. This image, was restored using ARCGIS software to get a shape file with the position of the Johnsons glacier front (see Table 4), once the picture is rectified to a horizontal plane at sea level, using a projective transformation (Shan, 1999).

In February 2007 an image was captured by the Quickbird system (DOCU 5) which covers the entire work area (missing some insignificant Northwest rocky outcrop). It is a raster file format GEOTIFF UTM 20S on the ellipsoid WGS84. Its original name is 07FEB03135449-M2AS-052422572010_01_P001.TIF and was obtained from http://www.euspaceimaging.com. It is an RGB color image with 16-bit digital values and an extra layer of near-infrared to 16 bits, but actually quantization levels are reduced to 11 bits. This image, was restored using ARCGIS software to get a shape file with the position of the Johnsons glacier front and Las Palmas lobe (see Table 5). This picture is rectified too to a horizontal plane at sea level, using a projective transformation.

From 2000 to 2012, the GSNCI has made scientific work on Hurd Peninsula, obtaining the position of the different glaciers fronts using GNSS techniques or theodolite. Sometimes the front was measured using a pole on the front line (Argentina, Las Palmas and Sally Rocks) with Real Time Kinematics (RTK) techniques (Blewitt, 1997). At other times, the antenna was in a backpack operator thus obtained accuracies were lower. Different shape files obtained in ARCGIS can be seen in Table 6.

| **Filename** | **Year** | $\sigma_{xy}$ **(m)** | **Geomatic adquired method** |
|---|---|---|---|
| CNDP-ESP_SIMRAD_FRONT_JOHNSON_1957.shp | 1957 | ±0,60 | Photogrammetric restitution, DOCU 1. |
| CNDP-ESP_SIMRAD_FRONT_SALLY_1957.shp | 1957 | ±1,20 | Photogrammetric restitution, DOCU 1. |
| CNDP-ESP_SIMRAD_FRONT_LAS_PALMAS_1957.shp | 1957 | ±1,20 | Photogrammetric restitution, DOCU 1. |
| CNDP-ESP_SIMRAD_FRONT_ ARGENTINA _1957.shp | 1957 | ±1,20 | Photogrammetric restitution, DOCU 1. |

*Table 2. Shape files obtained in ARCGIS for the flight made by BAS in 1957. In the third column the mean square error is shown.*

| **Filename** | **Year** | $\sigma_{xy}$ **(m)** | **Geomatic adquired method** |
|---|---|---|---|
| CNDP-ESP_SIMRAD_FRONT_JOHNSON_1990.shp | 1990 | ±2,00 | Photogrammetric restitution, DOCU 2. |
| CNDP-ESP_SIMRAD_FRONT_SALLY_1990.shp | 1990 | ±2,00 | Photogrammetric restitution, DOCU 2. |
| CNDP-ESP_SIMRAD_FRONT_LAS_PALMAS_1990.shp | 1990 | ±2,00 | Photogrammetric restitution, DOCU 2. |
| CNDP-ESP_SIMRAD_FRONT_ ARGENTINA _1990.shp | 1990 | ±2,00 | Photogrammetric restitution, DOCU 2. |

*Table 3. Shape files obtained in ARCGIS for the flight made by UKHO in 1990. In the third column the mean square error is shown.*

| **Name** | **Year** | $\sigma_{xy}$ **(m)** | **Geomatic adquired method** |
|---|---|---|---|
| CNDP-ESP_SIMRAD_FRONT_JOHNSON_2010.shp | 2010 | ±0,60 | Aereal photo, DOCU 4. |

*Table 4. Shape file obtained in ARCGIS and corresponding to the aerial photograph of QUICKBIRD system program (2010). In the third column the mean square error is shown. In this case, the image is corrected to sea level to obtain the correct planimetric position of the Johnsons glacier front.*

| **Name** | **Year** | $\sigma_{xy}$ **(m)** | **Geomatic adquired method** |
|---|---|---|---|
| CNDP-ESP_SIMRAD_FRONT_JOHNSON_2007.shp | 2007 | ±2,30 | Aereal photo, DOCU 5. |

| | | | |
|---|---|---|---|
| CNDP-ESP_SIMRAD_FRONT_LAS_PALMAS_2007.shp | 2007 | ±2,30 | Aereal photo, DOCU 5. |

*Table 5. Shape files obtained in ARCGIS and corresponding to the aerial photograph of QUICKBIRD system program (2007). In the third column the mean square error is shown. In this case, the image is corrected to sea level to obtain the correct planimetric position of the glacier fronts.*

| Name | Year | $\sigma_{xy}$ (m) | Geomatic adquired method |
|---|---|---|---|
| CNDP-ESP_SIMRAD_FRONT_SALLY_2000_2001.shp | 2000 | ±0,07 | GNSS pole, DOCU 6. |
| CNDP-ESP_SIMRAD_FRONT_SALLY_2004_2005.shp | 2005 | ±0,60 | GNSS backpack, DOCU 6. |
| CNDP-ESP_SIMRAD_FRONT_SALLY_2005_2006.shp | 2006 | ±0,60 | GNSS backpack, DOCU 6. |
| CNDP-ESP_SIMRAD_FRONT_SALLY_2007_2008.shp | 2008 | ±0,07 | GNSS pole, DOCU 6. |
| CNDP-ESP_SIMRAD_FRONT_SALLY_2008_2009.shp | 2009 | ±0,60 | GNSS backpack, DOCU 6. |
| CNDP-ESP_SIMRAD_FRONT_SALLY_2009_2010.shp | 2010 | ±0,07 | GNSS pole, DOCU 6. |
| CNDP-ESP_SIMRAD_FRONT_SALLY_2010_2011.shp | 2011 | ±0,07 | GNSS pole, DOCU 6. |
| CNDP-ESP_SIMRAD_FRONT_SALLY_2011_2012.shp | 2012 | ±0,07 | GNSS pole, DOCU 6. |
| CNDP-ESP_SIMRAD_FRONT_LAS_PALMAS_2000_2001.shp | 2000 | ±0,07 | GNSS pole, DOCU 6. |
| CNDP-ESP_SIMRAD_FRONT_LAS_PALMAS_2004_2005.shp | 2005 | ±0,60 | GNSS backpack, DOCU 6. |
| CNDP-ESP_SIMRAD_FRONT_LAS_PALMAS_2005_2006.shp | 2006 | ±0,60 | GNSS backpack, DOCU 6. |
| CNDP-ESP_SIMRAD_FRONT_LAS_PALMAS_2007_2008.shp | 2008 | ±0,07 | GNSS pole, DOCU 6. |
| CNDP-ESP_SIMRAD_FRONT_LAS_PALMAS_2008_2009.shp | 2009 | ±0,60 | GNSS backpack, DOCU 6. |
| CNDP-ESP_SIMRAD_FRONT_LAS_PALMAS_2009_2010.shp | 2010 | ±0,07 | GNSS pole, DOCU 6. |
| CNDP-ESP_SIMRAD_FRONT_LAS_PALMAS_2010_2011.shp | 2011 | ±0,07 | GNSS pole, DOCU 6. |
| CNDP-ESP_SIMRAD_FRONT_LAS_PALMAS_2011_2012.shp | 2012 | ±0,07 | GNSS pole, DOCU 6. |
| CNDP-ESP_SIMRAD_FRONT_ ARGENTINA _2000_2001.shp | 2000 | ±0,07 | GNSS pole, DOCU 6. |
| CNDP-ESP_SIMRAD_FRONT_ ARGENTINA _2004_2005.shp | 2005 | ±0,60 | GNSS backpack, DOCU 6. |
| CNDP-ESP_SIMRAD_FRONT_ ARGENTINA _2005_2006.shp | 2006 | ±0,60 | GNSS backpack, DOCU 6. |
| CNDP-ESP_SIMRAD_FRONT_ ARGENTINA _2007_2008.shp | 2008 | ±0,07 | GNSS pole, DOCU 6. |
| CNDP-ESP_SIMRAD_FRONT_ ARGENTINA _2008_2009.shp | 2009 | ±0,60 | GNSS backpack, DOCU 6. |
| CNDP-ESP_SIMRAD_FRONT_ ARGENTINA _2009_2010.shp | 2010 | ±0,07 | GNSS pole, DOCU 6. |
| CNDP-ESP_SIMRAD_FRONT_ ARGENTINA _2010_2011.shp | 2011 | ±0,07 | GNSS pole, DOCU 6. |
| CNDP-ESP_SIMRAD_FRONT_ARGENTINA_2011_2012.shp | 2012 | ±0,07 | GNSS pole, DOCU 6. |

*Table 6. Shape files obtained in ARCGIS and corresponding to the GSNCI inventory data. In the third column the mean square error is shown. In this case, the shape files are for Argentina, Las Palmas and Sally Rocks lobes front. GNSS techniques are applied to obtain these data.*

| Name | Year | $\sigma_{xy}$ (m) | Geomatic adquired method |
|---|---|---|---|
| CNDP-ESP_SIMRAD_FRONT_JOHNSON_2013.shp | 2013 | ±0,70 | Photogrammetric restitution, DOCU 7. |

*Table 7. Shape file obtained in ARCGIS and corresponding to the photogrammetric restitution from the Johnsons glacier front in February 2013. The picture was obtained with a non-metric camera.*

Finally the photogrammetric survey obtained in February 2013 with a non-metric camera (DOCU 7) for Johnsons Glacier front (see Table 7).

**Historical evolution of glacier fronts**

a) Johnsons Glacier

We operate with ARCGIS program to obtain the position of Johnsons Glacier front (at its intersection with the sea) along different years, as shown in Figure 9. From an analysis of these data it follows that the front glacier advanced 74 m in the central area (segment A) between 1957 and 1990. Then the front glacier retreated 171 m (sum of the segments A, L and F) between 1990 and 2007 to remain stable until 2010 and again to advance their central 31 m (segment L) between 2010 and 2013. Although located in 2013 ahead of his position in 2010 in this central position of the glacier front, you can see that in the south of the front changes trend and a setback of 57 m (segment J) between 2010 and 2013. Finally, note that, in the north, the glacier front has receded over 97 m between 1957 and 2013 (E segment). Near E segment the position of the front could be wrong but if we use the picture X26FID0093015 obtained at the beginning of 1957 (Rodríguez, 2014) from an incomplete British Antarctic Survey (BAS) photogrammetric flight (Figure 8a and 8b) we can see that this terminus line for the glacier is correct.

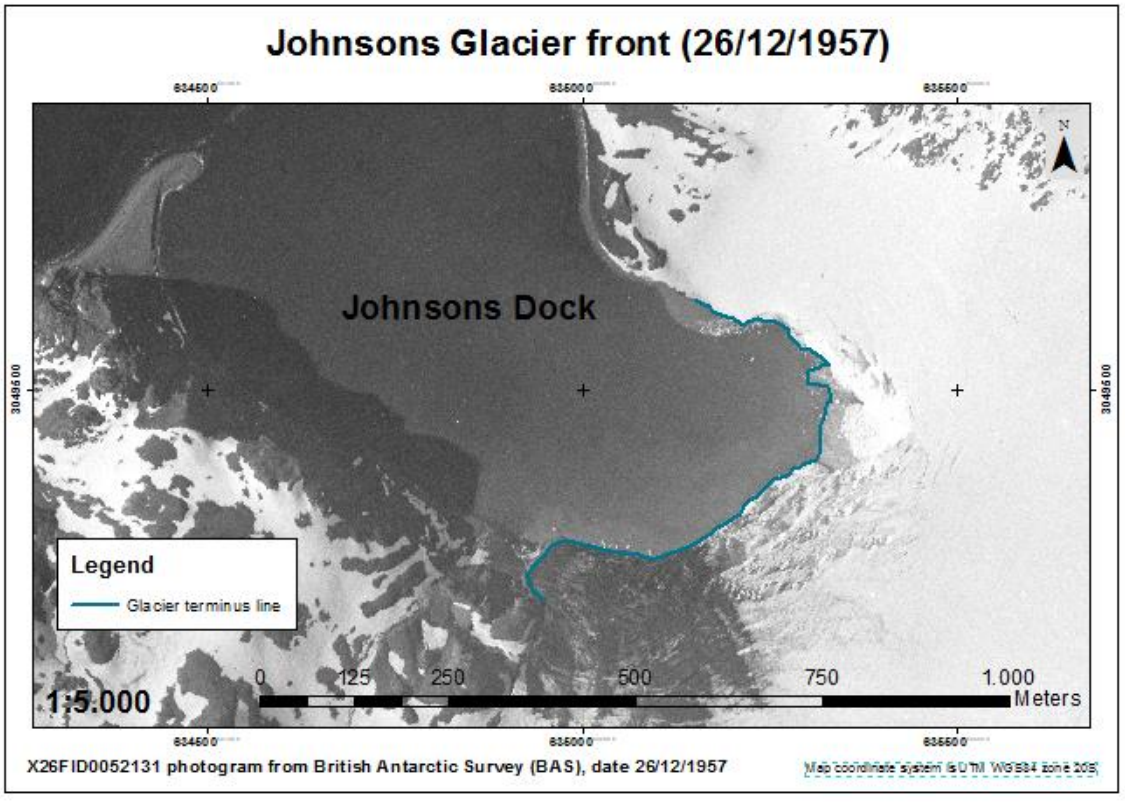


*Figure 8a. Terminus line for Johnsons Glacier (blue line) at the end of 1957. The base map corresponds to the BAS photogrammetric flight (date 26/12/1957).*

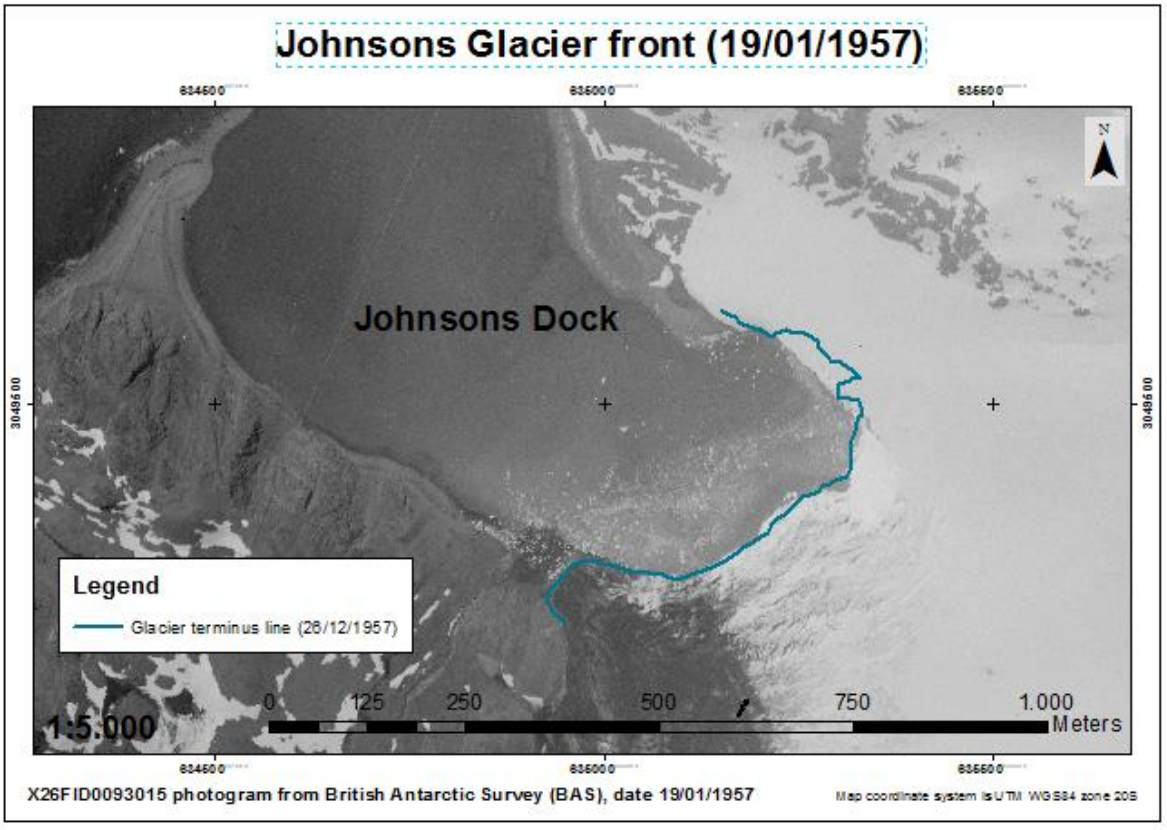


*Figure 8b. Terminus line for Johnsons Glacier (blue line) at the end of 1957. The base map corresponds to the BAS photogrammetric flight (date 19/01/1957). This flight is not completed and it only can be used for planimetry measurements at sea level.*

b) Sally Rocks lobe (Hurd Glacier)

Using the ARCGIS program and analyzing the position taken by the front along the years, as shown in Figure 10, it follows that the front glacier retreated 116 m in its central area (segment A) between 1957 and 1990. Then retreated 60 m (segment B) between 1990 and 2000, to rewind back to another 47 m (C segment) in 2000-2006 and another 36 m (D segment) from 2006 to 2009. From that date, has remained stable until 2012.

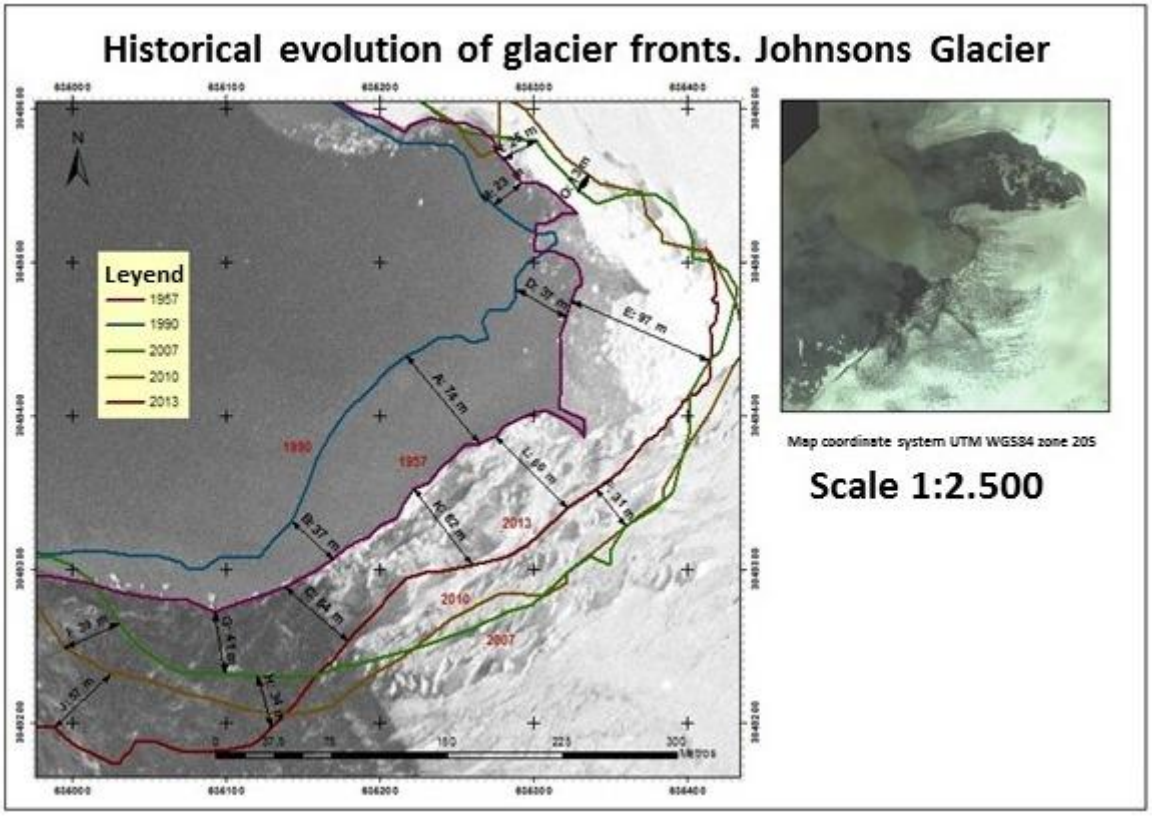


*Figure 9. History of the position of the Johnsons Glacier front. The oldest front position which data are available is 1957 (in purple) and the latest for the year 2013 (in red). The base map corresponds to the aerial photograph taken in 1957 by the BAS. The scale on which the figure does not match the map scale. The small image on the right side, corresponds to Quickbird (03/02/2007)*

c) Las Palmas lobe (Hurd Glacier)

As shown in Figure 11, the position taken by the front along the years follows that the front retreated 11 m in the central area (segment A) between 1957 and 1990. Then, the front retreated 24 m (segment F) between 1990 and 2000, to rewind back to another 17 m from 2000-2005 and another 14 m (D segment) from 2005 to 2007. From that date, has retreated another 10 m (although in other parts has been made) until 2009, to remain stable thereafter. Most striking in this case is that the decline experienced by the front between 1957 and 1990 is less pronounced than in the case of the front of Sally Rocks. This is mainly because in 1957 the glacier ended at sea and had to lose weight for height, until it began to recede on the beach and accentuate its reverse speed.

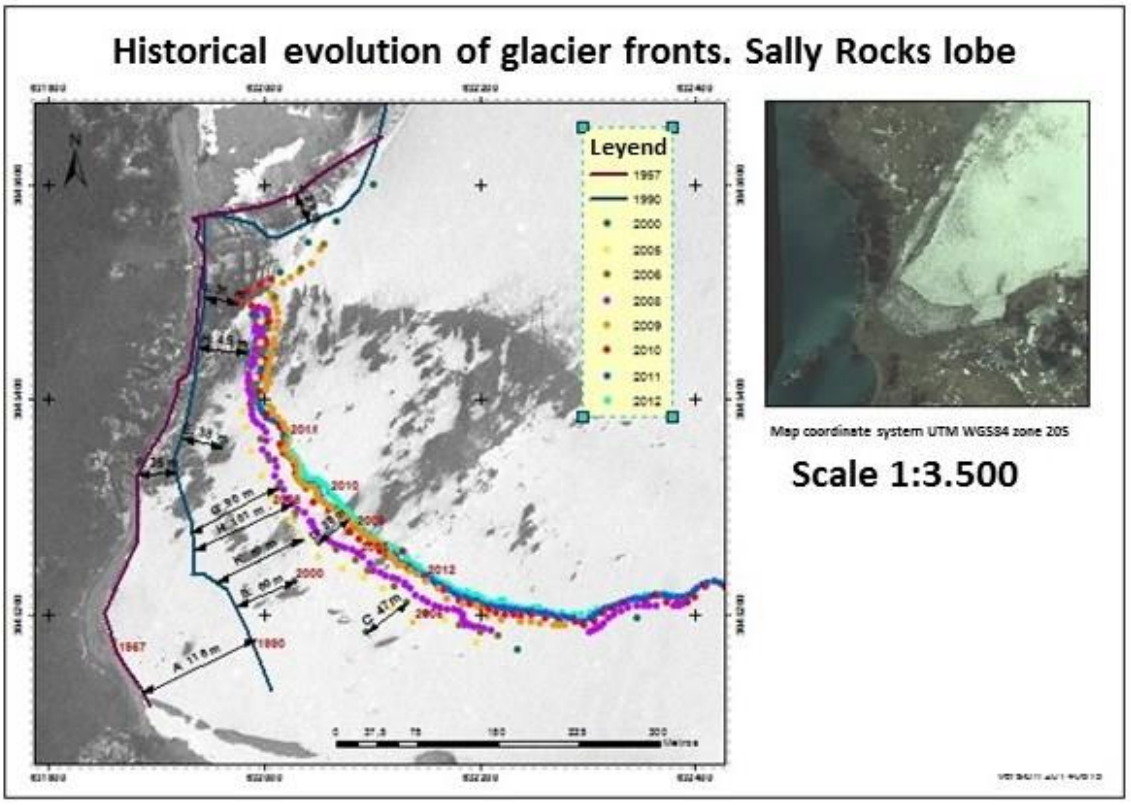


*Figure 10. Historical evolution of the position of Sally Rocks lobe front (Hurd Glacier). The oldest front position which data are available is 1957 (in purple) and the latest for the year 2012 (points in cyan). The base map corresponds to the aerial photograph taken in 1957 by the BAS. The scale on which the figure does not match the map scale. The small image on the right side, corresponds to Quickbird (03/02/2007)*

d) Argentina lobe (Hurd Glacier)

Analyzed the position taken by the front along different years in ARCGIS, as shown in Figure 12, it follows that the front glacier advanced 5m in its central area (segment A) between 1957 and 1990. Then the front retreated 70 m (A + B) from 1990-2000, to rewind back to another 15 m (C segment) in 2000-2005 and another 6 m from 2005 to 2008. From that date the front has retreated another 14 m (segment I) until 2009, to remain stable after this date, with slight losses. It is striking the slight advance of the front between 1957 and 1990.

Finally Figure 13a and Figure 13b show the evolution for the snout (Johnsons Glacier and Sally Rock lobe). The base map corresponds to 1990.

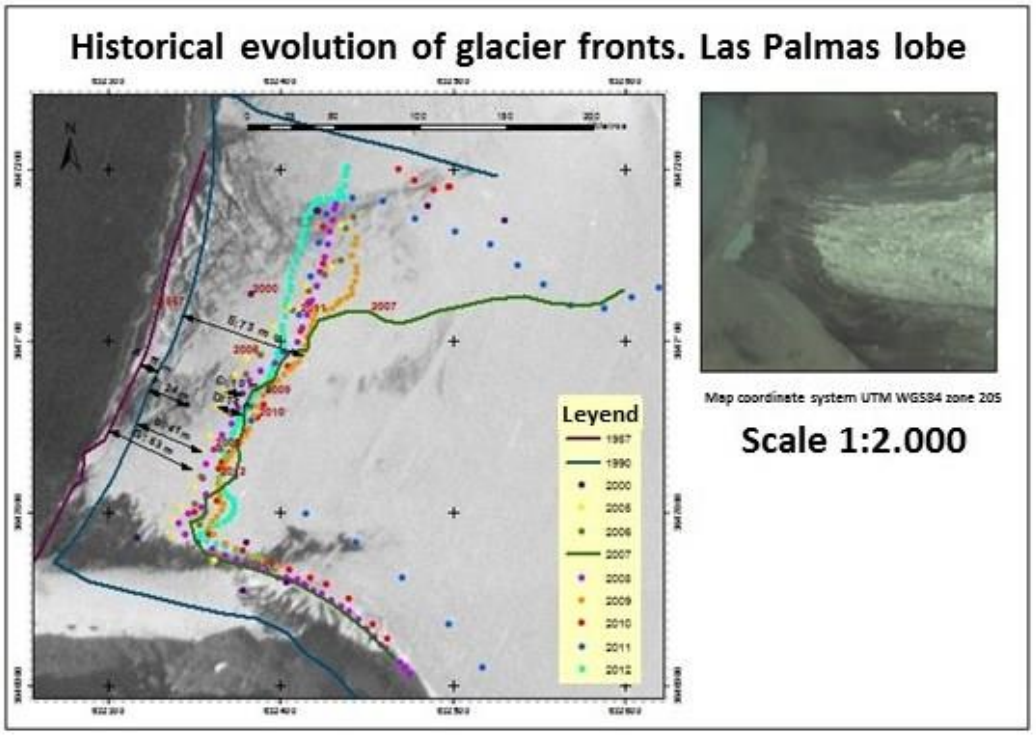


*Figure 11. Historical evolution of the position of the Las Palmas lobe front (Hurd Glacier). The oldest front position which data are available is 1957 (in purple) and the latest for the year 2012 (points in cyan). The base map corresponds to the aerial photograph taken in 1957 by BAS. The scale on which the figure does not match the map scale. The small image on the right side, corresponds to Quickbird (03/02/2007)*

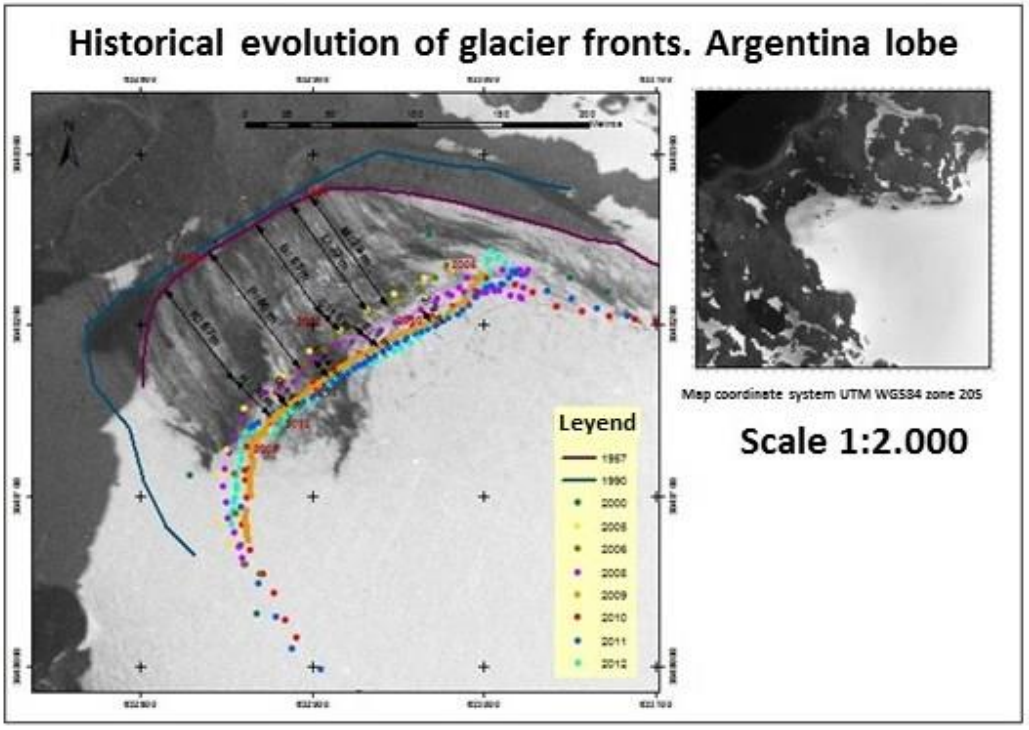


*Figure 12. Historical evolution of the position of Argentina lobe front (Hurd glacier). The oldest front position which data are available is 1957 (in purple) and the latest for the year 2012 (points in cyan). The base map corresponds to the aerial photograph taken in 1957 by the BAS. The scale on which the figure does not match the map scale. The small image on the right side, corresponds to Quickbird (29/01/2010)*

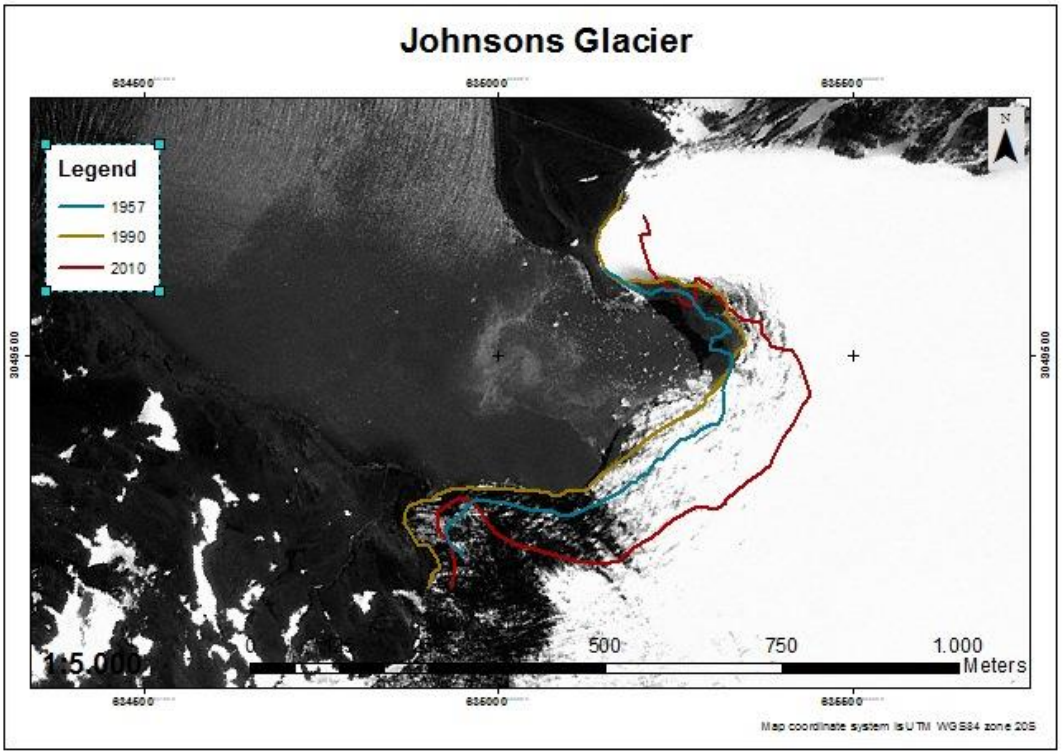


*Figure 13a. Historical evolution of the position of the snout (Johnsons Glacier). The base map corresponds to UKHO (United Kingdom Hydrographic Office, January 1990)*

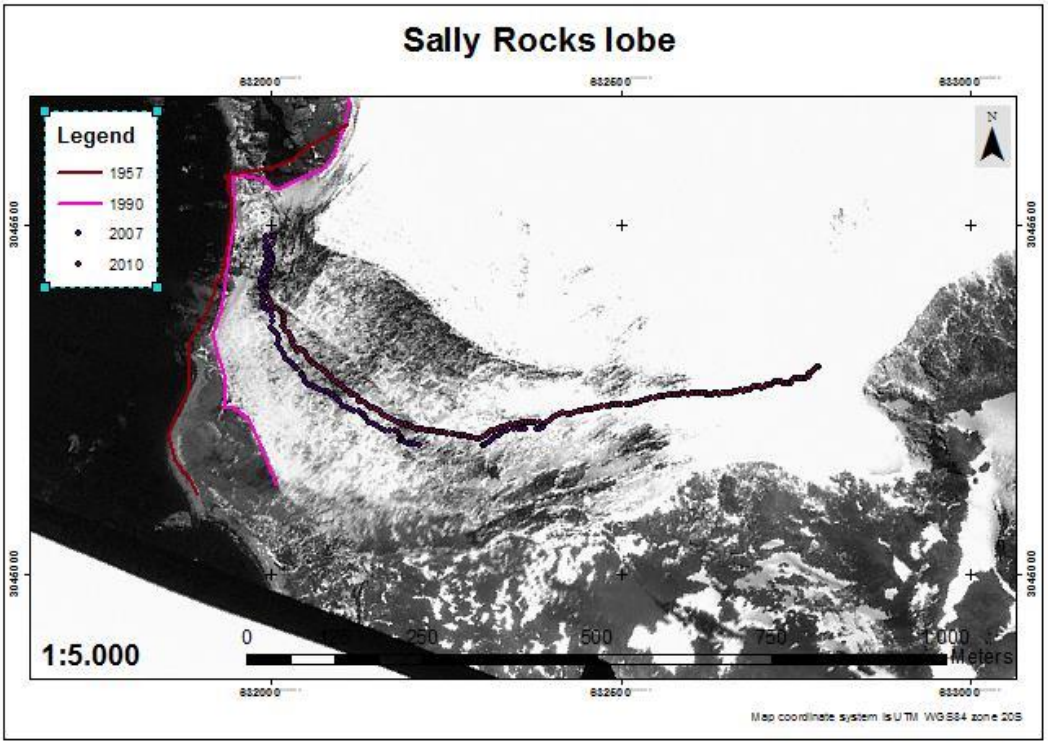


*Figure 13b. Historical evolution of the position of the snout (Sally Rocks lobe). The base map corresponds to UKHO (United Kingdom Hydrographic Office, January 1990). For 2007 and 2010 the terminus was delimitated using GNSS techniques.*

## Conclusions

- The close range photogrammetry with non-metric cameras is a very wise for technical jobs where it is not possible to access the study area, since it implies a lowering in cost without accuracy will suffer, compared with the use of metric cameras or laser scanner systems (much higher costs). In addition, the production of different products, such as digital surface models, linear flat, bent, orthophotos, virtual three-dimensional reproductions, etc., makes the presentation of results and facilitate decision making greatly.
- Johnsons front glacier (ends at sea resulting in the production of icebergs) saw a breakthrough in the middle of his forehead between 1957 and 1990, to suffer a subsequent decrease (greater than experienced forward) between 1990 and 2010. Between 2010 and 2013, suffered a slight increase; its final position in 2013 is 140 m behind it occupied in 1990.
- Argentina lobe front (nearest from Johnsons) has a slight increase from 1957-1990, to experience a sharp decline between 1990 and 2000. From this last year, has moderated its decline until 2010, in which virtually has stabilized. The central position of the front has fallen a total of 100 m from 1990-2012.
- Las Palmas lobe front, continued setback occurs in the time period analyzed, being more pronounced between 1990 and 2009, when it seems stable. The central position of the front has fallen a total of 84 m from 1957-2012. In 1957 this glacier ended at sea and had to lose weight for height, until it began to recede on the beach and accentuate its reverse speed.
- Finally, in the case of the Sally Rocks lobe front, continued setback occurs in the time period analyzed, being more pronounced between 1990 and 2010, when it seems to stabilize. The central position of the front has fallen a total of 259 m between 1957 and 2012.
- Of all fronts studied, which lies further south (Sally Rocks) is he who has suffered a major setback. Also noteworthy indicate that the biggest drop fronts occurred between 1990 and 2010.
- Analysis of the position of the different fronts it follows that from the year 2010, the pushback suffered all has stabilized.

## References


- Blewitt, G. (1997). *Basics of the GPS Technique: Observation Equations*. Department of Geomatics, University of Newcastle. United Kingdom.
- Brown, D.C. (1971). *Close-range camera calibration*, PE&RS, Vol. 37(8), pp.855-866.
- Domínguez, F. (1993). Topografía general y aplicada, Ediciones Mundi-Prensa.
- Kraus, K. (2007). *Photogrammetry* Geometry from Images and Laser Scans, 2nd Ed., de Gruyter.
- Kraus, K. (1993). Photogrammetry, Vol. 1: Fundamentals and Standard Processes, Dümmlers.
- Luhmann, T., Robson, S., Kyle, S. and Harley, I. (2006). *Close Range Photogrammetry. Principles, techniques and applications.* Whittles Publishing.
- Molina, C., Navarro, F., Calvet, J., García-Selles, D. and Lapazaran, J. (2007). *Hurd península glaciers, Livingston Island, Antarctica, as indicators of regional warming: ice-volume changes during period 1956-2000.* Ann. Glaciol. 46 (1), 43-49.
- Navarro, F.J., Jonsell, U.Y., Martín, A. and Rodríguez, R. (2011). *Diez años de medidas balance de masas en los glaciares Johnsons y Hurd (Isla Livingston, Antártida) revelan que su pérdida de masa no se ha acelerado durante el último decenio*, VIII Simposio de Estudios Polares. Palma de Mallorca,7-9 septiembre de 2011.
- Navarro, F., Jonsell, U., Corcuera, M., and Martín-Español, A. (2013). *Decelerated mass loss of Hurd and Johnsons glaciers, Livingston Island, Antarctic Peninsula*, J. Glaciol., 59, 115–128.
- Palà, V., Calvet, J., García Sellés, D. y Ximenis, L. (1999). *Fotogrametría terrestre en el Glaciar Johnsons, Isla Livingston, Antártida*, Acta Geológica Hispánica, v. 34, nº 4, pp. 427-445.
- Rodríguez, R. (2014). *Integración de modelos numéricos de glaciares y procesado de datos de georradar en un sistema de información geográfica*, Tesis Doctoral. Universidad Politécnica de Madrid, pp. 235-242.
- Shan, J.J. (1999). *A Photogrammetric Solution for Proyective Reconstruction*. Department of Geomatics Engineering. Purdue University. SPIE Conference on Vision Geometry VIII. Denver, Colorado. 296-304.

- Wolf, P.R. (1983). *Elements of Photogrammetry with Air Photo Interpretation and Remote Sensing*. Second Edition. McGraw-Hill Book Company. New York, N.Y.